IAC-24-A6.4.8.x85823

Thermite-for-Demise (T4D): Numerical and experimental description of the pressure build-up in an enclosed volume

Alessandro Finazzi[a1]*, Jacopo Domaschio[b], Alberto Verga[c], Filippo Maggi[d], Alessandro Turchi[e]

[a] *Dept. of Aerospace Science and Technology, Politecnico di Milano, via La Masa, 34, Milan (MI), 20156, Italy,* alessandro.finazzi@polimi.it
[b] *Dept. of Aerospace Science and Technology, Politecnico di Milano, via La Masa, 34, Milan (MI), 20156, Italy,* jacopo.domaschio@mail.polimi.it
[c] *Dept. of Aerospace Science and Technology, Politecnico di Milano, via La Masa, 34, Milan (MI), 20156, Italy,* alberto.verga@polimi.it
[d] *Dept. of Aerospace Science and Technology, Politecnico di Milano, via La Masa, 34, Milan (MI), 20156, Italy,* filippo.maggi@polimi.it
[e] *Agenzia Spaziale Italiana, Via del Politecnico s.n.c., Rome (RM), 00133, Italy,* alessandro.turchi@asi.it
* Corresponding Author

Abstract

The space debris population around the Earth is growing more and more every year, and it is necessary to foresee appropriate countermeasures. The main mitigation action for LEO objects is the atmospheric re-entry, whose principal drawback is the inevitable casualty risk on ground. Among the possible technologies to limit this hazard, the use of thermite charges to enhance the spacecraft demise during the process is currently under investigation. One of the main concerns related to this concept is the possible pressure build-up after the thermite ignition, which could imply challenges in the on-ground verification in wind tunnels and, in a real application during re-entry, result in an uncontrolled fragmentation of the spacecraft. A dedicated experimental facility was realized to characterize the pressure generated by a thermite reacting in a confined volume, even in near-vacuum conditions. An ignition strategy based on induction heating was selected to ensure the complete and reliable ignition of the charge. A mechanically activated Al/Cu_2O mixture was used for these tests. TG/DTA analysis was used to obtain the Arrhenius parameters of the selected thermite couple. The obtained results indicate that the peak pressure inside the closed volume is only slightly dependent on the initial chamber pressure. The open source Porous material Analysis Toolbox based on OpenFOAM (PATO) was selected to numerically reproduce the experiment. The numerical model proved to be suitable to describe the thermite ignition and combustion.

Keywords: Design-for-Demise, thermite, combustion, ignition, gas generation

Nomenclature

Variables

E_a	Activation energy	[kJ/mol]
α	Conversion degree	[-]
G	Gas generation	[-]
m	Mass	[kg]
l	Length	[mm]
A	Pre-exponential factor	[1/min]
Δp	Pressure peak	[atm]
r	Radius	[mm]

Pedices

ad	Adiabatic
F	Fluid
TMD	Theoretical Maximum Density
T	Thermite

Acronyms/Abbreviations

CNES	Centre national d'études spatiales
D4D	Design-for-Demise
DTA	Differential Thermal Analysis
ESA	European Space Agency
ISO	International Organization for Standardization
LEO	Low Earth Orbit
NASA	National Aeronautics and Space Administration
OFW	Ozawa Flynn Wall
PATO	Porous material Analysis Toolbox
T4D	Thermite-for-Demise
TGA	Thermal Gravimetric Analysis
ZVS	Zero Voltage Switching

1. Introduction

The more and more frequent news connected to spacecraft re-entry events is an indication of the urgency for space debris mitigation and remediation actions. After several decades in which the risks implied by space debris presence in Low Earth Orbit (LEO) were discussed only within the research community (e.g., the Kessler syndrome was postulated in 1978 [1]), recently the consequences of space pollution became evident even

for the general public. On August 28, the re-entry of a space object (later identified with a Starlink satellite) caused concerns in the population of Southern Germany and Switzerland, which called the police in several cities after having seen an unexpected glow in the sky [2]. In other cases, space debris were effectively able to reach the ground endangering people and goods: for example, on March 8 2024 a battery survived the atmospheric re-entry and hit a house in Naples, Florida [3]. In the sole North America, two other similar cases were reported during spring 2024 [4][5]. One of the most straightforward strategies to avoid (or at least limit) the casualty risk on ground is to design the space systems such that their ablation during the re-entry process is maximized. This design rationale, named Design-for-Demise (D4D), is now a suggested approach in the NASA [6] and ISO [7] standards, and the preferred one for ESA missions [7].

D4D can be applied to spacecraft of limited mass to lower the expected casualty risk to an acceptable value, hereby enabling an uncontrolled re-entry. Moreover, in a broader sense, this design methodology can be useful as well for spacecraft needing a controlled re-entry, as it can limit the aftermath consequent to a failed manoeuvre. Many D4D techniques have been proposed in the last decade and are currently under research [9].

A peculiar D4D approach is the inclusion of exothermic materials on board aiming to increase the available enthalpy for the demise process. Upon re-entry, the reactive material should be able to be passively ignited by the aerothermal heat experienced by the space object and act as a source of additional enthalpy. The best candidate material for this role is thermite; for this reason, this D4D concept will be referred to as Thermite-for-Demise (T4D) in the present paper. Thermites are a subset of energetic materials and consist in mixtures of a metal and a metal oxide. The selection and the characteristics of the starting ingredients greatly influence the properties of the exothermic redox reaction that can be induced by an appropriate energetic trigger [10]. However, in general, thermites show high energetic density, high flame temperature, and self-sustaining rection. An appropriate selection of the mixture can lead to the desired properties in terms of cost, toxicity, safety, and gas generation. Moreover, this class of pyrotechnics contains both fuel and oxidizer, and is for this reason suitable for applications in harsh environments (e.g., in space or underwater).

To date, research on T4D is still limited. The concept was proposed by CNES in a patent in 2011 [11], and later expanded by another one filed by ESA in 2018 [12]. Four experimental campaigns in high-enthalpy hypersonic wind tunnels were performed to prove the technology [13]-[16]. In all these tests, the pyrotechnic charge was either encapsulated in a vessel or inserted in the structural voids of a space hardware mock-up. The ability of the thermite of perforating a titanium plate or inducing partial demise on a simple steel mock-up was successfully verified. However, one of the main difficulties during the tests was the management of the pressure generated in the closed volume, which could lead to the ejection of unreacted material or, in case of catastrophic failure, to the uncontrolled fragmentation f the object. In fact, even if thermochemical computations can provide the gas generation that should be expected by an adiabatic thermite reaction in standard conditions, the effects of uncomplete combustion and of sub-atmospheric external pressure are difficult to predict.

In this paper, the pressure generated by a thermite reacting in closed configuration will be explored experimentally and numerically. In Section 2 the tested material will be detailed, together with the experimental line and the numerical model used to represent its combustion, based on OpenFOAM PATO [17]. The obtained results will be presented and discussed in Section 3, while the main conclusions and the outlook for future research will be reported in Section 4.

2. Material and methods

2.1 Thermite production

The thermite used in this study is a stoichiometric mixture of Al and Cu_2O, in loose form, mechanically activated to increase its reactivity. In this work, this thermite formulation was assumed to undergo a one-step reaction as per Eq. 1.

$$2Al + 3Cu_2O \rightarrow Al_2O_3 + 6Cu \quad (1)$$

The characteristics of this formulation and of the reaction described by Eq. 1, in case of theoretical combustion in standard conditions, are reported in Table 1. The starting ingredients used to realize the thermite are described in Table 2. These powders were mixed in stoichiometric ratio and mechanically activated following the patented NHEMA procedure [18] to grant reliable and fast ignition in the setup described in Section 2.2.2.

Table 1. Theoretical properties of Al/Cu2O mixture [10]

React.	ρ_{TMD} [g/cm^3]	T_{ad} [K]	G [-]	-Q [J/kg]
2Al + $3Cu_2O$	5.280	2843	0.078	2.408E6

Table 2. Starting powders characteristics

Ingredient	Particle size	Purity	Supplier
Al	30 µm	≥99%	AMG Alpoco
Cu_2O	<5 µm	97%	Sigma Aldrich

2.2 Experimental methods

2.2.1 TG/DTA

The Al/Cu_2O thermite combustion was assumed to behave as a first order reaction. The Arrhenius parameters were obtained using TG/DTA, realized with a Netzsch STA 449 F5 Jupiter. The powder was heated up to 1100 °C at constant heating rate in air. Air atmosphere was selected to be consistent with the selected numerical case, that will be introduced in Section 2.3. Four samples of 15±0.1 mg were inserted in alumina (Al_2O_3) crucibles and processed at heating rates of 2.5, 5.0, 10.0, and 20.0 K/min. The Arrhenius parameters were then computed from the resulting TG/DTA curves using the Ozawa-Flynn-Wall (OFW) method [19][20].

2.2.2 Experimental line based on induction heating

An experimental line based on induction heating was developed to allow the measurement of the pressure trace of the reacting thermite and to ensure the complete ignition of the powder. In each test, 200 mg of powder were used. The pyrotechnic charge was placed inside a 304 stainless steel cylindrical pressure vessel, closed at one end. At the other end, the vessel was connected to a pressure transducer and a ball valve which can either connect the pipe system to a vacuum pump or to the environment. At its ends, the cylindrical container was characterized by two circular fins. The total volume enclosed by the pressure chamber and the piping (up to the valve) was 8.52 ± 0.01 ml. The extremity of the pressure vessel where the thermite was lodged was heated by means of a commercially available zero voltage switching induction heating circuit with nominal power output of 1000 W. The circular fins were introduced in the design to increase the coupling between the electromagnetic field and the thermite vessel. Their dimension was selected to reproduce a realistic heating rate of an atmospheric re-entry. The temperature of the walls of the vessel was monitored through a 2-colour pyrometer and a modified K-type thermocouple. The thermocouple was shielded from the electromagnetic field to avoid interference, as suggested in [21]. The pyrometer signal was acquired via USB and the computer software provided by the manufacturer, while the thermocouple was interfaced with a data logging board. A comprehensive list of the equipment is reported in Table 3. The complete scheme of the system is shown in Fig. 1, while the temperature profile that can be obtained with this setup in the area of the thermite lodgement is presented in Fig. **2**.

2.3 Numerical method

The numerical model used to describe the thermite combustion is OpenFOAM PATO [17]. PATO is an open-source modular analysis platform for multiphase porous reactive materials distributed by NASA. It was originally developed to simulate the thermal response of thermal protection materials. Its numerical models are principally devoted to pyrolysis processes, in which the thermal decomposition of the material induces an outgassing. The numerical model is obtained by volume-averaging the governing equations for the conservation of mass, species/elements, momentum, and energy.

As thermites are porous reactive materials, usually producing limited amount of gas upon reaction, the description provided by PATO is coherent with the physics of the phenomenon. For this reason, PATO was selected to describe the experiments presented in this paper. However, while in pyrolysis the endothermic decomposition process and the gas production are simultaneous and coupled, in thermite reactions the heat

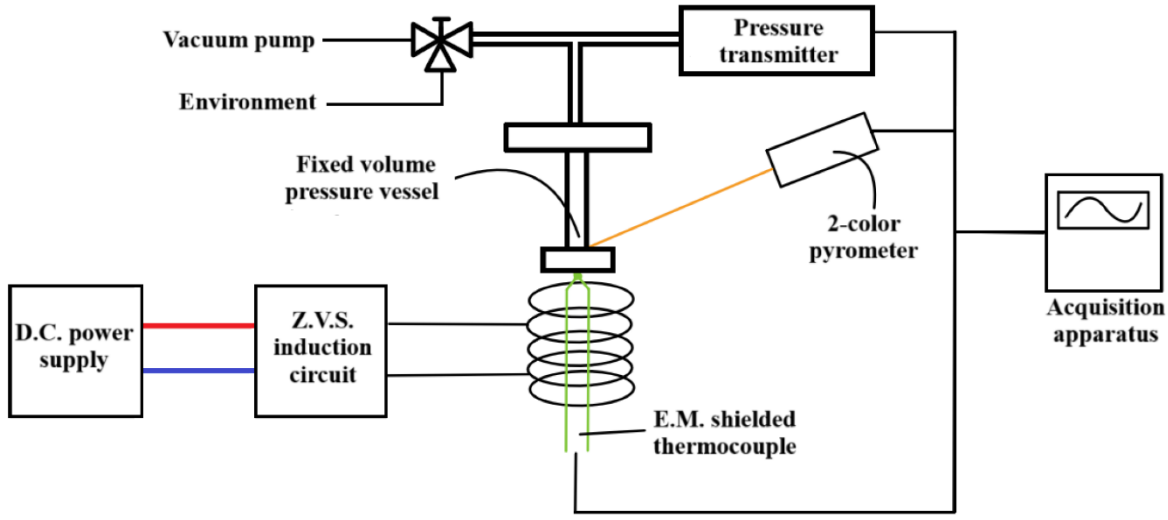

Fig. 1. Induction-based experimental line for the measurement of the pressure generated by a reacting thermite

and gas release are not so strictly tied. For example, there are thermites that do not release enough enthalpy to provoke the gasification of one of the reaction products (e.g., Al/SiO_2 or Ti/Fe_2O_3). In this work, this discrepancy was neglected and the heat release due to the thermite reaction was considered simultaneous to the subsequent gas production. The simulation presented in this paper aims at rebuilding the tests performed in standard air atmosphere.

Table 3. Components of the pressure measurement experimental line

Component	Manufacturer and model
Pressure transmitter	Trafag ref. 8472.25.8917
Pyrometer	IMPAC Igar 6 Adv.
Thermocouple	TC Direct K-type
Oscilloscope	Tektronix DPO2014
Data logger	PicoLog TC-08
ZVS circuit	Unbranded, P.R.C. made
Power supply	Bosytro DY-48V1000W

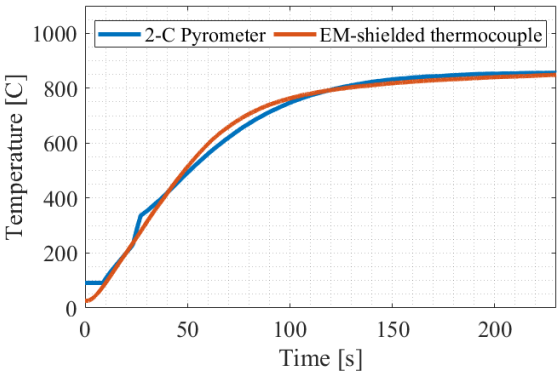

Fig. 2. Temperature profile of the thermite vessel in the area of thermite lodgement

2.3.1 Case setting

The geometry of the combustion chamber introduced in Section 2.2.2 was simplified to a cylinder consisting of two regions: a first one representing a porous reactive media (the thermite) and a second one representing the air volume contained in the experimental line. Being an axisymmetric geometry, only a wedge of 2.5° of the domain was simulated. A scheme of the case geometry is shown in Fig. 3, while its dimensions are reported in Table 4. The characteristic length of the cells was respectively of the order of 0.03 mm in the thermite region and of 0.5 mm in the fluid region. The maximum Courant number imposed through the simulation was equal to 0.5. However, a maximum timestep of 3e-7 s was imposed to appropriately capture the thermite reaction; for this reason, the Courant number during the simulation was generally lower than 10^{-3}. Due to the very low timestep value, it was not possible to simulate the complete heating process of the thermite vessel as depicted in Fig. **2**. For this reason, the temperature boundary condition applied on the external walls of the thermite region was a simple ramp, starting from 300 K at the beginning of the simulation and reaching 1100 K after 0.1 s, which was the total duration of the simulation. The external walls of the fluid region were assumed not to heat during the test; thus, their temperature was maintained to 300 K during the whole simulation. The other boundary conditions used in the simulation are reported in Table 5.

The initial temperature of the whole geometry was set to 300 K, while the initial pressure of the fluid to 101325 Pa. The fluid was considered laminar during the simulation and characterized with the properties of air.

2.3.2 Thermite representation

The thermite was represented as a porous reactive material with negligible volume fraction of fibres, that was set to 0.01. In the adopted scheme, the virgin material represented the unreacted formulation (Al/Cu_2O) while the char material was associated with the products of the thermite reaction (Al_2O_3/Cu). Therefore, the thermochemical data of these materials was obtained by weighting the data of the single chemical species considering a stoichiometric formulation. The thermochemical properties of the involved chemical species were taken from the NIST webbook [28]. Similarly, the gas produced by the thermite reaction was assumed to be pure Cu. The gas generation imposed to the chemical reaction was equal to the one computed by Fischer and Grubelich [10] (Table 1), as well as the theoretical maximum density of the virgin material. The volume fraction of the virgin material was set to 0.3 to represent the loose state of the charge used in the tests. The sole reaction considered in this simulation was the thermite combustion (Eq. 1), characterized by the kinetic parameters obtained through the TG/DTA measurements presented in Section 3.1. The material sub-models used in the simulation are shown in Table 6.

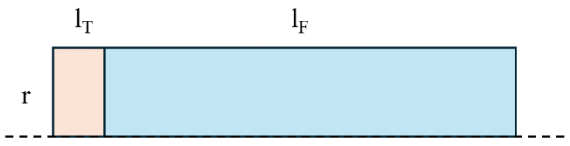

Fig. 3. Scheme of the numerical simulation geometry

Table 4. Dimensions of the geometry for the numerical simulation

Dimension	Value
Radius, r	6.77 mm
Thermite length, l_1	0.88 mm
Fluid length, l_2	58.32 mm

Table 5. Boundary conditions used in the simulated test case

Field	Boundary	Condition
Temperature	Thermite external walls	Ramp, 300 K to 1100 K in 0.1 s
	Thermite to fluid	turbulentTemperatureRadCoupledMix
	Fluid external walls	Constant (300 K)
	Fluid to thermite	turbulentTemperatureRadCoupledMix
Pressure	Thermite external walls	zeroGradient
	Thermite to fluid	turbulentTemperatureCoupledBaffleMixed
	Fluid external walls	zeroGradient
	Fluid to thermite	turbulentTemperatureCoupledBaffleMixed
Density	All	zeroGradient
Velocity	All	noSlip

Table 6. Material sub-models used in the simulation

Model	Thermite
Pyrolysis	LinearArrhenius
Mass	DarcyLaw
Energy	Pyrolysis
Gas Properties	Tabulated
Material Properties	Porous
Time Control	GradP

3. Results and discussion

3.1 TG/DTA

The results of the TG/DTA performed in air at various heating rates on the Al/Cu_2O thermite are shown in Fig. 4. The mass of the sample increases in three distinct ramps, spaced out by plateaus. The first ramp, ranging from 300 to 500 °C, corresponds to a 10% increment in mass. This can be explained by the oxidation of Cu_2O to 2CuO, which would give exactly a 9.32% increment over the original thermite mass. This reaction is justified by the fact that CuO is the most stable oxide of copper at ambient pressure in this temperature range [22].

The second ramp occurs in concomitance with the exothermic peak caused by the thermite reaction. The mass increase could be due to the oxidation of the metal product and/or the creation of other compounds such as the spinel $CuAl_2O_4$, already observed in previous research [23]. Similar considerations can be made for the third ramp.

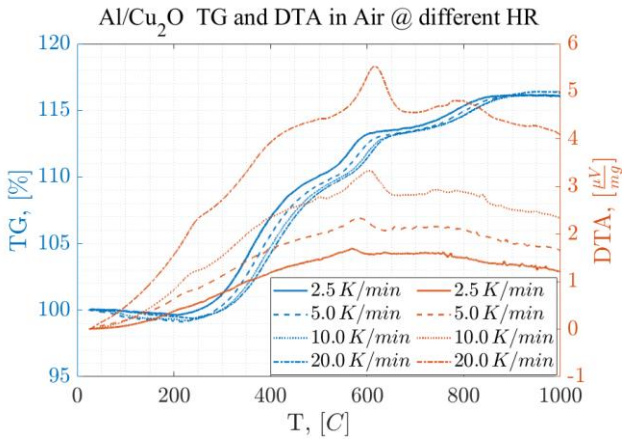

Fig. 4. TG/DTA curves in air at different heating rates of the Al/Cu_2O activated thermite

From these results, the OFW method was applied to obtain the Arrhenius parameters of the thermite combustion, assuming a first-order reaction. Values of conversion degree α spanning from 0.1 up to 0.9 were considered. The start of the reaction process (α=0) was set to 200 °C. Below this temperature, any mass loss was attributed to moisture or acetone evaporation. The end of the thermite reaction (α=1) was identified with the plateau at 700 °C, after the exothermic peak that can be seen in the DTA curves. Therefore, the sample mass m_α at a certain conversion degree α can be expressed as per Eq. 2:

$$m_\alpha = \alpha(m_{700} - m_{200}) + m_{200} \quad (2)$$

Where m_{700} and m_{200} are respectively the mass recorded by the balance at 700 and 200 °C, for each heating rate. Following the procedure described in [20], it the activation energy, E_a, and the pre-exponential

factor, *A*, were computed. The results are presented in Fig. 5.

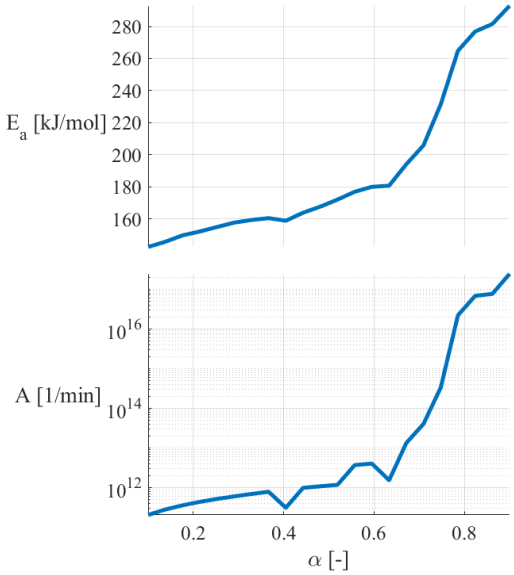

Fig. 5. Kinetic parameters of the Al/Cu_2O thermite reaction at different conversion degree

3.2 Pressure measurement tests

Each ignition test performed in the induction-based experimental line resulted in a graph like the one shown in Fig. 6. After a slight increase in pressure due to the vessel heating, a spike in the pressure curve can be observed. It is important to highlight that in these conditions, the recorded peak is broad and multiple points with the highest-pressure value can be appreciated. This indicates that the resolution of the pressure sensor is adequate.

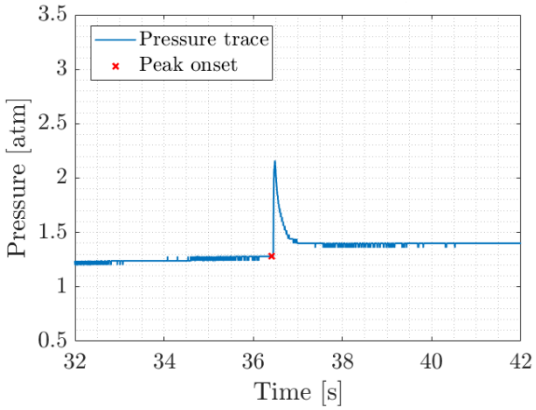

Fig. 6. Pressure trace of the thermite reaction, in a test performed with initial atmosphere pressure equal to 1 atm

3.2.1 Peak amplitude

The peak amplitude, defined as the difference between the peak and onset pressure, was registered for several values of initial chamber pressures. The obtained values are reported in Fig. 7. For all the tests, the measured pressure peak amplitude was in the range between 0.4 and 1 atm. This value seems almost independent on the initial chamber pressure. A slight influence of the initial chamber pressure can be seen, resulting in an increase of the peak amplitude for higher initial pressures. However, the R^2 of this correlation is poor. This contrasts with the thermochemical computations presented by Monogarov et al. [24], which predict a higher gas production for thermite reactions at lower ambient pressure. A possible explanation can be found in considering the trade-off of two different effects. On the one hand, low environmental pressure should favour the vaporization process. On the other hand, the law of mass action for gas phase reactions states that the reaction rate is proportional to the product of the partial pressure of the reactants elevated to their respective stoichiometric coefficients [25]. Consequently, the kinetics of the reaction are faster if the partial pressure in the confined geometry is higher. This consideration could explain the higher-pressure peak registered for higher initial chamber pressure.

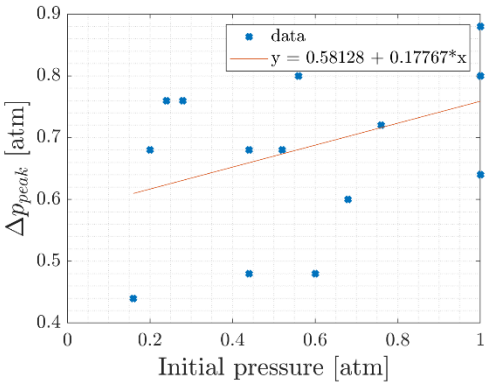

Fig. 7. Pressure peak amplitude as a function of the initial chamber pressure (R^2 = 0.14279)

3.2.2 Residual pressure

It has been observed that, after the combustion chamber had cooled down to room temperature, a non-negligible over-pressure with respect to the initial one was present inside. This residual pressure has been recorded and reported in Fig. 8. This effect cannot be provoked by the theoretical products of the thermite reactions (Cu and Al_2O_3) which would condensate once the vessel cools down. Instead, this pressurization could be attributed to the partial decomposition of the oxidizer and its consequent oxygen release. It is reported in the literature that thermites can release O_2 during their combustion process and even before their main redox reaction [26]. From the data shown in Fig. 8, it seems that low environmental pressure favours the release of O_2. This is in accordance with previous literature [27]. These observations could partially explain the results presented

in Fig. 7. The escaped oxygen may have not taken part in the redox reaction, lowering the overall enthalpy released by the thermite. Therefore, less gaseous products could have been produced by the thermite reaction and less enthalpy could have been transferred to the air surrounding the thermite. This would have led to an overall lower pressure peak.

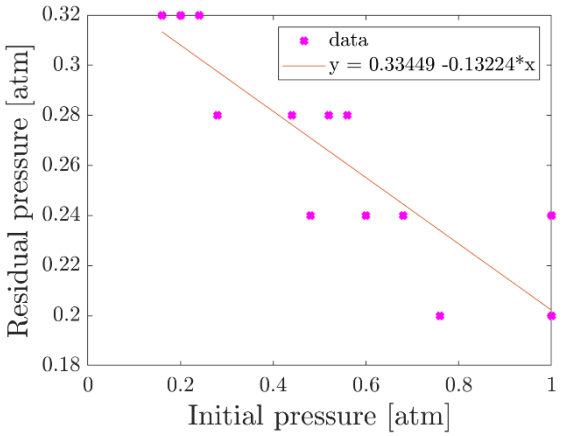

Fig. 8. Residual pressure in the combustion chamber after the test as a function of the initial chamber pressure (R^2 = 0.7929). The apparent discrete behaviour of this measurement is due to the limited resolution of the pressure sensor

3.2.3 Expelled mass

After the tests, a considerable amount of condensed metal was observed on the underside of the combustion chamber cap (Fig. 9). For this reason, the lower part of the combustion chamber was weighted immediately before and after each test. The estimate of the expelled mass obtained in this way is presented in Fig. 10 together with the linear regression of the experimental data. In the same figure, the theoretical gas generation prediction by Fischer and Grubelich [10] is shown as well: this value, even if computed only for combustion in standard conditions and not equivalent to the expelled mass, can be considered as a reference. These results should be considered with caution, as the procedure is prone to errors (e.g., some material could have condensed on the lateral walls of the combustion chamber). The expelled mass estimated in this way was higher for lower initial chamber pressure, and in general significantly higher than the theoretical prediction. The results presented in Fig. 10 suggest that the expelled mass cannot be a consequence of the sole condensation of gasified reaction products. The entrainment of liquid droplets in the gas generated by the reaction and their successive deposition on the underside of the combustion chamber cap seems a more realistic hypothesis. The entrained droplets would have encountered less resistance in the more rarefied atmosphere, therefore explaining the greater amount of expelled mass associated to the tests with lower starting chamber pressure.

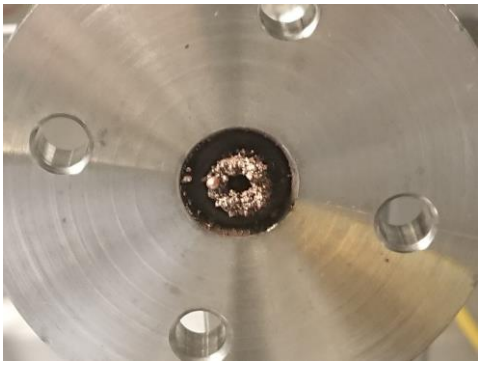

Fig. 9. Appearance of the underside of the combustion chamber cap after the tests

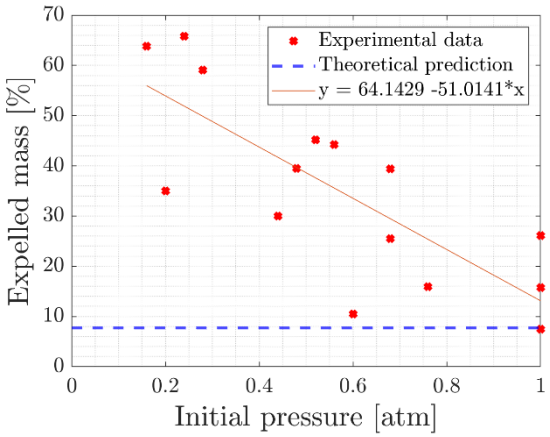

Fig. 10. Expelled mass recorded during the experimental campaign, theoretical gas generation prediction by Fischer and Grubelich [10], and linear regression of the experimental data (R^2 = 0.60842)

3.3 OpenFOAM PATO simulation

The values of the activation energy and pre-exponential factor corresponding to a conversion factor of 0.5 were selected for the numerical simulation. This choice led to an activation energy of 170 kJ/mol and to a pre-exponential factor of $1e10^{12}$ 1/min. The main results of the simulation are presented in Fig. 11 and Fig. 12. As it can be seen in Fig. 11, the simulated thermite material onset was equal to 909 K. This ignition temperature is coherent with the results of the TG/DTA measurements presented in Section 3.1. The difference with the experimental values can be explained by the choice of using constant values for the activation energy and pre-exponential factor. The maximum temperature reached during the simulation was 3108 K. This value is higher than the adiabatic flame temperature that can be computed using thermochemical data (Table 1). This result is probably due to the insufficient time

discretization. However, this inaccuracy was deemed acceptable to avoid an excessive computational burden.

The maximum pressure registered during the simulation in the fluid region is shown in Fig. 12. The simulated peak amplitude was of about 0.03 atm, significantly lower than the experimental values previously presented in Section 3.2.1. This is probably due to the boundary condition adopted between the porous medium and the fluid. With the current setup, the pressure generated by the thermite is averaged with the pressure level of the fluid region at the interface. On the one hand, this coupling is necessary to represent the physical connection between the two regions. On the other hand, the pressure levels reached in the bulk of the thermite are more similar to the ones measured experimentally, and this similitude is lost once the dumping boundary condition is applied. A new boundary condition formulation could overcome this limit.

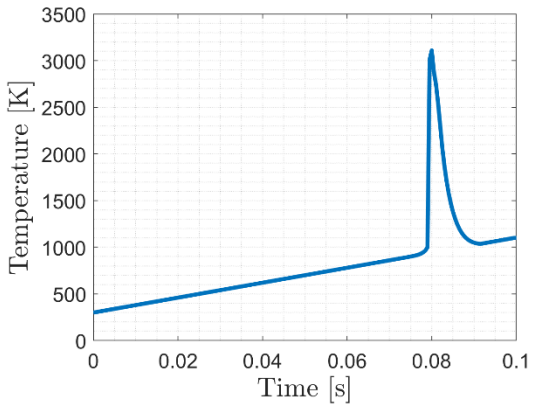

Fig. 11. Maximum temperature in the thermite region during the simulation

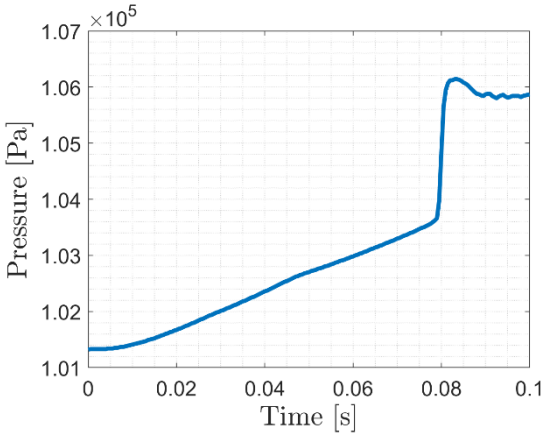

Fig. 12. Maximum pressure in the fluid region during the simulation

4. Conclusions

In this work, the study of the gas generation of thermites was deepened from both an experimental and a numerical point of view. An innovative pressure measurement experimental line based on induction heating has been presented. This ignition strategy ensures the complete ignition of the thermite charge, so that a clear connection between the reacting powder mass and the measured pressure peak can be derived. Moreover, the design of the experimental line consented to operate in a near-vacuum environment and at a heating rate representative of an atmospheric re-entry. The selected thermite for the pressure tests was an activated Al/Cu2O stoichiometric mixture. This powder was characterized through TG/DTA in air in order to estimate its Arrhenius parameters, under the hypothesis of first-order reaction. The results obtained from the pressure measurement tests indicate that the dependance of the generated pressure peak on the initial chamber pressure is weak. For higher initial chamber pressure, slightly higher-pressure peaks were recorded. After the tests, a residual pressure of the combustion chamber was observed. It is hereby suggested that prior to the thermite reaction, the partial decomposition of the oxidizer results in the emission of oxygen, which is partially unable to react with the fuel. This could explain why the pressure peak slightly decreases for lower initial chamber pressure, which facilitates the decomposition of the oxidizer. Moreover, the mass expelled from the lower part of the combustion chamber appears to increase slightly for lower initial chamber pressure. This could be due to the lower drag experimented by the liquid droplets entrained in the gas generated by thermite. Lastly, an innovative application of the open-source OpenFOAM PATO numerical model was explored. The tests performed in standard atmosphere were rebuilt numerically to prove the capability of the software to describe the ignition and combustion of porous, energetic materials. Relying on the Arrhenius parameters computed from TG/DTA, the ignition of the pyrotechnic material was reproduced numerically with satisfying accuracy. The maximum temperature registered in the simulation was slightly higher than the adiabatic flame temperature derived from thermochemical computations, but it is expected that a finer time resolution would lead to a maximum value consistent with that result. In the simulated case, the pressure peak obtained was significantly lower than the one measured experimentally. It is hereby suggested that a different strategy on the coupling boundary conditions between the porous, reactive material and the surrounding fluid could lead to a more precise representation of the tests results.

Acknowledgements

Part of the research presented in this paper has been performed in the framework of the 2023 “Internship Programme” initiative between the Agenzia Spaziale Italiana and the Space Generation Advisory Council.

Both institutions are gratefully acknowledged for their support.

List of references

[1] D.J. Kessler, B.G. Cour-Palais, Collision Frequency of Artificial Satellites: The Creation of a Debris Belt, Journal of Geophysical Research 83 (1978) 2637–2646, DOI: 10.1029/JA083iA06p02637.

[2] SWI swissinfo.ch, Mysteriöser Schweif – Experten: Satellit statt Meteorit, 28 August 2024, https://www.swissinfo.ch/eng/science/mysteri%C3%B6ser-schweif-experten-satellit-statt-meteorit/87449881, (accessed 02.09.24).

[3] J. Wattles, NASA says it expected space station garbage to burn up. The debris smashed into a Florida home instead, 24 April 2024, https://edition.cnn.com/2024/04/16/world/space-junk-florida-home-crash-scn/index.html, (accessed 02.09.24).

[4] M. Liverman, On remote trail, man stumbles upon heavy, mysterious object possibly from outer space, 24 May 2024, https://wlos.com/news/local/haywood-county-man-finds-heavy-mysterious-object-possibly-outer-space-landed-remote-trail-canton-aerospace-expert-input-glamping-collective, (accessed 02.09.2024).

[5] A. Stewart, Sask. farmers baffled after finding strange object in prairie field, 10 May 2024, https://regina.ctvnews.ca/from-outer-space-sask-farmers-baffled-after-discovering-strange-wreckage-in-field-1.6880353, (accessed 02.09.24).

[6] Anon., Process for Limiting Orbital Debris. Tech. rep. NASA-STD-8719.14C, National Aeronautics and Space Administration, 2021.

[7] Anon., Space systems - Space debris mitigation requirements. Tech. rep. BS ISO 24113:2023. Inter-Agency Space Debris Coordination Committee, 2023.

[8] AA. VV., ESA Space Debris Mitigation Requirements, Tech. rep. ESSB-ST-U-007, Issue 1, Revision 0. European Space Agency, 2023.

[9] B.M. Cattani, A. Caiazzo, S. Lemmens, L. Innocenti, An Overview of Design for Demise Technologies, 8th European Conference on Space Debris, Darmstadt, Germany, 2021.

[10] S.H. Fischer, M.C. Grubelich, Theoretical energy release of thermites, intermetallics, and combustible metals, Proceedings of the 24th International Pyrotechnics Seminar, Monterey, California, USA, 1998.

[11] D. Dihlan, P. Omaly, Élement de véhicule spatial a capacité d'autodestruction ameliorée et procedure de fabrication d'un tel element, French patent 2975080B1, 2011.

[12] R. Seiler, G. Smet, Exothermic reaction aided spacecraft demise during reentry, European patent 3604143A1, 2018.

[13] K.A. Monogarov, I.N. Melnikov, S.M. Drozdov, D. Dilhan, Yu.V. Frolov, N.V. Muravyev, A.N. Pivkina, Pyrotechnic approach to space debris destruction: From thermal modeling to hypersonic wind tunnel tests, Acta Astronautica 172 (2020) 47-55, DOI: 10.1016/j.actaastro.2020.03.028.

[14] T. Schleutker, A. Gülhan, B. Esser, T. Lips, ERASD - Exothermic Reaction Aided Spacecraft Demise - Proof of Concept Testing, Technical report ERASD_TR. DLR, Supersonic and Hypersonic Technologies Department, 2019.

[15] B. Lockett, Demisability of Non-demisable Spacecraft Constituents, Space Mechanisms Workshop on Clean Space, Noordwijk, The Netherlands, 2024.

[16] A. Finazzi, D. Daub, F. Maggi, C. Paravan, S. Dossi, T. Lips, G. Smet, K. Bodjona, Thermite-for-demise (T4D): Experiments and numerical modelling on ball-bearing unit mock-ups containing thermite in an arc-heated wind tunnel, Acta Astronautica 223 (2024) 550-576, DOI: 10.1016/j.actaastro.2024.06.013.

[17] J.E.B. Meurisse, J. Lachaud, N.N. Mansour, PATO User Guide. Version 3.1, National Aeronautics and Space Administration, 2022.

[18] S. Dossi, C. Paravan, F. Maggi, G. Colombo, L. Galfetti, A method for the mechanical activation of powders by means of balls. Patent WO 2019/102345 A1, 2019.

[19] X. Zhang, Applications of Kinetic Methods in Thermal Analysis: A Review, Engineered Science 14 (2021) 1-13.

[20] Anon., Standard Test Method for Decomposition Kinetics by Thermogravimetry Using the Ozawa/Flynn/Wall Method, ASTM E1641-16, 2016.

[21] C. Mou, P. Y. Nabhiraj, Capturing the Temperature of the Workpiece in an Induction Heating System Using Thermocouple with Minimal Error, 5th International Conference on Electronics, Materials Engineering and Nano-Technology (IEMENTech), Kolkata, India, 2021.

[22] J. P. Neumann, T. Zhong, Y. A. Chang, The Cu-O (Copper-Oxygen) System. Bulletin of Alloy Phase Diagrams 5:2 (1984) 136-140.

[23] W. Hu, F. Donat, S. A. Scott, J. S. Dennis, The Interaction between CuO and Al2O3 and the Reactivity of Copper Aluminates below 1000 °C and their Implication on the Use of the Cu–Al–O System for Oxygen Storage and Production, RSC Advances 6:113016 (2016).

[24] K. A. Monogarov, A. N. Pivkina, L. I. Grishin, Yu. V. Frolov, D. Dilhan, Uncontrolled Re-entry of

Satellite Parts After Finishing Their Mission in LEO: Titanium Alloy Degradation by Thermite Reaction Energy, Acta Astronautica 135 (2017) 69-75.

[25] L.T. De Luca, Energetic problems in aerospace propulsion - Notes for students, Grafiche GSS, Revised and Extended Preliminary Edition, Bergamo, Italy, 2008.

[26] K. Sullivan, M. R. Zachariah, Simultaneous Pressure and Optical Measurements of Nanoaluminum Thermites: Investigating the Reaction Mechanism. Journal Of Propulsion and Power 26:3 (2010) 467-472.

[27] L. Durães, R. Santos, A. Correia, J. Campos, A. Portugal, Thermal Behavior of Fe_2O_3/Al Thermite Mixtures in Air and Vacuum Environments, AIP Conference Proceedings 845:1 (2006) 956–959.

[28] National Istitute of Standards and Technology, NIST Chemistry WebBook, SRD 69, January 2023, https://webbook.nist.gov/chemistry/, (accessed 16.09.24).